ISSN: 2414-1895 DOI: 10.6919/ICJE.202305_9(5).0029

Vibration Isolation Analysis of Foundation under Harmonic Load using the FEM with PML

Kuankuan Chen

Department of Civil Engineering, Jiangsu University, Zhenjiang, Jiangsu, 212013, P.R. China

1070011050@qq.com

Abstract

A wave impeding block (WIB) vibration isolation barrier for foundation vibration isolation control is proposed, and its vibration isolation performance is numerically analyzed. Firstly, the control equation of the perfectly matched layer (PML) absorbing boundary is established in the frequency domain by using the complex coordinate stretching transformation. Secondly, using the Galerkin approximation technique, the frequency domain finite element formulation of the second-order non-splitting scheme PML with displacement as the basic unknown is given. Finally, the effects of modulus ratio, length, and load frequency on the vibration isolation performance of the WIB vibration isolation barrier are analyzed by numerical examples. The results show that the WIB vibration isolation barrier can effectively control the ground vibration caused by different frequency vibration sources.

Keywords

Wave Impeding Block; Perfectly Matched Layer; Finite Element; Vibration Isolation.

1. Introduction

Because the environmental vibration generated by vehicles and machines not only affects the quality of life of residents but also have a lot of adverse effects on the normal operations of precision instruments, vibration has been listed as one of the major environmental hazards in the world [1]. To effectively eliminate or reduce environmental vibrations has now become an important concern in civil engineering. Vibration isolation is undoubtedly one of effective approaches to deal with this problem. There are two kinds of vibration isolation methods, namely, the active vibration isolation method and passive vibration isolation method. For the active vibration isolation method, the vibration isolation is accomplished by using vibration isolation system to block energy transmission from the vibrational source to the surrounding medium, while for the passive vibration isolation method, the vibration isolation is realized by deploying vibration isolation facility around the protected structure to reduce the amount of energy delivered to the structure. So far, facilities such as the open trench, infilled trench, concrete wall, flexible gas mattress, WIB, and pile rows are used as vibration isolation systems for the passive vibration isolation.

Different from the vibration isolation mechanism of the empty trench, filling trench, and row pile, the WIB has obvious advantages in medium and low-frequency vibration control. Since Schmid et al. [2] proposed the concept of WIB, scholars have done a lot of research on WIB. Among them, Schmid et al. [2] and Takemiya et al. [3-5] analyzed the vibration isolation performance of WIB and pointed out that the WIB is a reliable vibration isolation measure. And the latter first proposed a honeycomb WIB and used field test research. The results show that the structure has better vibration isolation performance. Peplow et al. [6] used the boundary integral equation method to study the active vibration isolation effect of the two-dimensional double-layer foundation WIB and pointed out that

ISSN: 2414-1895 DOI: 10.6919/ICJE.202305_9(5).0029

the WIB has advantages in vibration control in the low-frequency range. Lombaert et al. [7] also concluded that the WIB plays an effective role in controlling the low-frequency vibration generated by rail transit. Celebi et al. [8] used a nonlinear two-dimensional finite element method to study the vibration isolation performance of WIB on ground vibration caused by rail transit and found that the design of WIB with a low impedance ratio can isolate vibration more effectively. Thompson et al. [9] used the boundary element method to study the vibration isolation performance of the WIB buried under the track. The results show that the WIB can effectively reduce the vibration between 16 and 50 Hz.

In this paper, based on the PML absorbing boundary, the vibration isolation performance and related influencing factors of the WIB vibration isolation barrier are analyzed and discussed by using the frequency domain finite element method.

2. Governing Equations for the Foundation

Considering that the foundation soil and WIB are homogeneous isotropic linear elastic materials, the momentum balance equation of elastic medium has the following expression

$$\sigma_{ij,j} + \rho\omega^2 u_i = 0, \tag{1}$$

in which u_i are the displacement components; σ_{ij} are the stress components; ρ is the density of the medium. The constitutive relation for the stresses of the elastic medium of the foundation is as follows

$$\sigma_{ij} = 2\mu\varepsilon_{ij} + \lambda e\delta_{ij}, \tag{2}$$

where ε_{ij} are the strain components; e is the dilatation of the elastic medium; δ_{ij} is the Kronecker delta; λ and μ are the Lame constants. The strain components of the elastic medium can be expressed by the displacement components as follows

$$\varepsilon_{ij} = \frac{1}{2}\left(u_{i,j} + u_{j,i}\right), \tag{3}$$

The constitutive relations for the frequency domain stresses can be obtained via equation(2) As

$$\sigma_{xx} = M_l\varepsilon_{xx} + \lambda\varepsilon_{yy}, \sigma_{yy} = M_l\varepsilon_{yy} + \lambda\varepsilon_{xx}, \sigma_{xy} = \mu\gamma_{xy}, \tag{4}$$

in which γ_{xy} is the shear strain. With equation(3), the strain components in equations (4) have the forms

$$\varepsilon_{xx} = \frac{\partial u_x}{\partial x}, \varepsilon_{yy} = \frac{\partial u_y}{\partial y}, \gamma_{xy} = \frac{\partial u_x}{\partial y} + \frac{\partial u_y}{\partial x} \tag{5}$$

As shown in equation(1), the inertial force of the elastic medium in the frequency domain has the form

$$f_i^{(1)} = \rho\omega^2 u_i. \tag{6}$$

3. The FE Equations with PML for the WIB

The FEM is a common numerical calculation method for solving complex problems. In the finite element numerical simulation of elastic wave scattering and dynamic response of WIB vibration isolation barrier in half space, due to the limitation of computer memory and calculation time, a limited space area must be intercepted for simulation, which naturally introduces artificial medium boundary. When the elastic wave reaches these boundaries, the meaningless boundary reflection wave field will directly affect the analysis and judgment of the problem. In order to weaken or eliminate the above effects, a certain boundary condition must be added to the boundary of the artificial medium, which is usually called the absorbing boundary condition. It is used to simulate the physical process of unidirectional wave propagation from the near-field finite field to the far-field infinite field through

ISSN: 2414-1895 DOI: 10.6919/ICJE.202305_9(5).0029

the artificial boundary without reflection. So far, a variety of absorbing boundary conditions have been widely used [10]. Among them, PML is a new absorbing boundary condition proposed by Berenger [11] in the calculation of electromagnetic wave problems. In theory, this method can completely absorb waves incident at any angle and any frequency, and has become the most effective absorbing boundary.

3.1 Governing Equations for the PML

To improve the accuracy of the FEM solution, a PML is introduced at the bottom and both sides of the FEM domain of the foundation. PML can absorb the incident wave from the truncated boundary of the FEM domain, thereby reducing the reflected wave from the boundary. The PML domain also needs to be discretized. In order to absorb the incident wave, the complex coordinates of the PML domain need to be introduced. Therefore, the following complex coordinate transformation is introduced for x-coordinate

$$\tilde{x} = \int_0^x \lambda_x(x)\,\mathrm{d}x, \tag{7}$$

where λ_x is the stretching functions in x-direction. For the derivatives along the x-direction, the following expressions can be obtained

$$\frac{\partial}{\partial \tilde{x}} = \frac{1}{\lambda_x(x)}\frac{\partial}{\partial x}. \tag{8}$$

By using equation (1), the equation of motion for the elastic medium in the PML is as follows

$$\sum_j \frac{1}{\lambda_j}\frac{\partial \sigma_{ij}}{\partial x_j} = -\rho\omega^2 u_i \tag{9}$$

Multiplying both sides of equation (9) by λ_x, one has the following equation of motion for the elastic medium

$$\sum_j \beta_j \frac{\partial \sigma_{ij}}{\partial x_j} = -\rho\omega^2 \lambda_x u_i,\ \beta_j = \lambda_m \lambda_n,\ m \neq n \neq j \tag{10}$$

In which β_j is independent of the coordinate x_j.

3.2 The FE Equations with PML for Foundation

Multiplying both sides of equation (10) by δu_i^* and integrating over the domain occupied by an elastic medium, the following virtual work principle with complex coordinate stretch for the x- coordinate is obtained

$$\int_V \sigma_{ij}\delta\varepsilon_{ij}^*\mathrm{d}v = \int_V \rho\omega^2 u_i \delta u_i^*\mathrm{d}v + \int_{\partial V} t_i\,\delta u_i^*\mathrm{d}s \tag{11}$$

in which δu_i^* is the virtual displacement components and $\delta\varepsilon_{ij}^*$ are the corresponding virtual strain components; t_i are the components of the traction acting on the boundary of the medium; the symbol * denotes the complex conjugate.The principle of element virtual work in the form of matrix is as follows

$$\int_{S_e} \delta\hat{\boldsymbol{\varepsilon}}^{*T}\hat{\boldsymbol{\sigma}}\mathrm{d}s = \int_{S_e} \delta\hat{\mathbf{u}}^{*T}\hat{\mathbf{f}}^{(\mathrm{I})}\mathrm{d}s + \int_{\partial S_e} \delta\hat{\mathbf{u}}^{*T}\hat{\mathbf{t}}\mathrm{d}l \tag{12}$$

in which V_e and ∂V_e denote the volume and boundary of the element; $\tilde{\boldsymbol{\sigma}}$, $\tilde{\mathbf{f}}^{(\mathrm{I})}$ and $\tilde{\mathbf{t}}$ are the stress vector, inertial force vector and traction vector of the element . Introducing the shape functions for the element, the displacement vector of the element can be represented by

ISSN: 2414-1895 DOI: 10.6919/ICJE.202305_9(5).0029

$$\hat{\mathbf{u}}^{(e)} = \left[\hat{u}_x^{(e)} \hat{u}_y^{(e)} \right]^T = \mathbf{N}^{(e)} \hat{\mathbf{u}}^{(e_d)}, \mathbf{N}^{(e)} = \left[\mathbf{N}^{(e,1)} \ \mathbf{N}^{(e,2)} \ \ldots \ \mathbf{N}^{(e,n_d)} \right],$$
$$\hat{\mathbf{u}}_{G_i}^{(e_d)} = \left[\hat{\mathbf{u}}_{G_i}^{(e,1)T} \ \hat{\mathbf{u}}_{G_i}^{(e,2)T} \ldots \hat{\mathbf{u}}_{G_i}^{(e,n_d)T} \right]^T, q = 1 \sim n_d \tag{13}$$

in which $\hat{\mathbf{u}}^{(e)}$ is the interpolated displacement vector for the element; $\hat{\mathbf{u}}^{(e_d)}$ and $\hat{\mathbf{u}}^{(e,q)}$ are the node displacement vector for the element and the displacement vector for the q-th node of the element; $\mathbf{N}^{(e)}$ is the shape function matrix for the element; n_d is the total number of the nodes of the element. Using the interpolated displacement vector as given by equation(5), and equation(13), the interpolated strain vector of the element has the form

$$\hat{\boldsymbol{\varepsilon}}^{(e)} = \left[\hat{\varepsilon}_{xx}^{(e)} \hat{\varepsilon}_{yy}^{(e)} \hat{\gamma}_{xy}^{(e)} \right]^T = \mathbf{B}^{(L_{\mathrm{I}})} \hat{\mathbf{u}}^{(e_d)} \tag{14}$$

where $\mathbf{B}^{(L_{\mathrm{I}})}$ is the strain matrix. Employing equations (4) and (14), the following representation for the interpolated stress vector is obtained

$$\hat{\boldsymbol{\sigma}}^{(e)} = \left[\hat{\sigma}_{xx}^{(e)} \hat{\sigma}_{yy}^{(e)} \hat{\sigma}_{xy}^{(e)} \right]^T = \sum \mathbf{D}^{(e)} \mathbf{B}^{(L_{\mathrm{II}})} \hat{\mathbf{u}}^{(e_d)} \tag{15}$$

in which $\mathbf{D}^{(e)}$ is the elasticity matrix for the element and $\mathbf{B}^{(L_{\mathrm{II}})}$ is another strain matrix. Since the virtual displacements $\delta\hat{\mathbf{u}}^{(e_d)}$ of the element nodes are arbitrary, the following finite element equation for the element in the PML associated with the i-th harmonic wave is hence deduced

$$\sum \mathbf{k}^{(e)} \hat{\mathbf{u}}^{(e_d)} - \omega^2 \sum \mathbf{m}^{(e)} \hat{\mathbf{u}}^{(e_d)} = \hat{\mathbf{f}}^{(e)}, \mathbf{k}^{(e)} = \int_{S_e} \mathbf{B}^{(L_{\mathrm{I}})T} \mathbf{D}^{(e)} \mathbf{B}^{(L_{\mathrm{II}})} \mathrm{d}s,$$
$$\mathbf{m}^{(e)} = \rho^{(e)} \int_{S_e} \lambda_x \mathbf{N}^{(e)T} \mathbf{N}^{(e)} \mathrm{d}s, \hat{\mathbf{f}}^{(e)} = \int_{\partial S_e} \mathbf{N}^{(e)T} \mathbf{t}^{(e)} \mathrm{d}l \tag{16}$$

in which $\mathbf{k}^{(e)}$ and $\mathbf{m}^{(e)}$ are the stiffness and mass matrices of the element for the case of the three-node element; $\hat{\mathbf{f}}^{(e)}$ is the equivalent node load vector for the element.

4. Numerical Analysis

4.1 The Influence of Load Frequency on the Dynamic Response of WIB Vibration Isolation System

This section studies the influence of load frequency on the dynamic response of the WIB vibration isolation system. The bedrock is assumed to be rigid, and only one soil layer is assumed to be covered on the bedrock. Fig.1 is the vibration isolation system diagram of the WIB. The abscissa of the center of the WIB is 0m, the harmonic point load is (x, y) = (-6.5m, 0m), and the coordinate of the observation point is (x, y) = (0.5m, 0m). The PML boundary is applied on both sides of the vibration isolation system, the outer boundary of PML is free, and the bottom of the system is fixed. The material and geometric parameters of WIB and soil are shown in Table.1 The frequency range of the harmonic point load is [0Hz, 50Hz], and 101 sample points are evenly distributed on it. In the finite element simulation, the three-node element is used to discretize the vibration isolation system in the x and y directions. The calculation area of the finite element simulation in this section, the size of the x-direction triangular element is 0.5m, which is divided into 88 elements, and the size of the y-direction element is also 0.5m, which can be divided into 30 elements. Therefore, the finite element calculation area is divided into 5280 units. The shear modulus of WIB and soil is given by the Cole-Cole model. According to the Cole-Cole model [12], the shear modulus of the material of the vibration isolation system can be obtained as follows :

$$\mu(\omega) = \mu_\infty \frac{1 + \chi(i\beta\omega)^{-\alpha}}{1 + (i\beta\omega)^{-\alpha}} = \mu_\infty + \frac{\mu_\infty(\chi - 1)}{1 + (i\beta\omega)^{\alpha}}, \chi = \frac{\mu_0}{\mu_\infty}, 0 < \alpha < 1, \chi \le 1, \tag{17}$$

ISSN: 2414-1895 DOI: 10.6919/ICJE.202305_9(5).0029

where $\mu(\omega)$ is the frequency-dependent complex shear modulus; μ_∞ is the limit of the complex shear modulus for $\omega \to \infty$, and μ_0 is the value of the complex shear modulus for $\omega \to 0$; β is a characteristic relaxation time and α controls the width of the transition zone between μ_∞ and μ_0. It can be seen from Fig.2 that when the harmonic point load frequency exceeds 20 Hz, the horizontal displacement and vertical displacement at the observation point will hardly change. When the load frequency is about 3Hz, the response of horizontal displacement and vertical displacement reaches the peak and then decreases sharply, indicating that the vibration isolation effect of WIB is significant in the low frequency range, but the vibration isolation effect is not ideal in the middle and high frequency bands.

Table 1. The material and geometric parameters for the WIB and soil

Parameters	Symbols	Values	Units
Densities of the WIB and soil	ρ_w, ρ_s	3.0×10^3, 2.0×10^3	kg/m^3
Shear moduli of the WIB and soil	$\mu_{w\infty}$, $\mu_{s\infty}$	1.2×10^{10}, 2.0×10^7	Pa
Poisson's ratio of the WIB and soil	ν_w, ν_s	0.2, 0.3	
Parameter χ in the Cole-Cole model for the WIB and soil	χ_w, χ_s	0.9, 0.75	
Parameter α in the Cole-Cole model for the WIB and soil	α_w, α_s,	0.5, 0.5	
Parameter β in the Cole-Cole model for the WIB and soil	β_w, β_s,	5×10^{-3}, 5×10^{-2},	
The thickness of the overlying soil layer	H	15	m
Length of the WIB	d		m

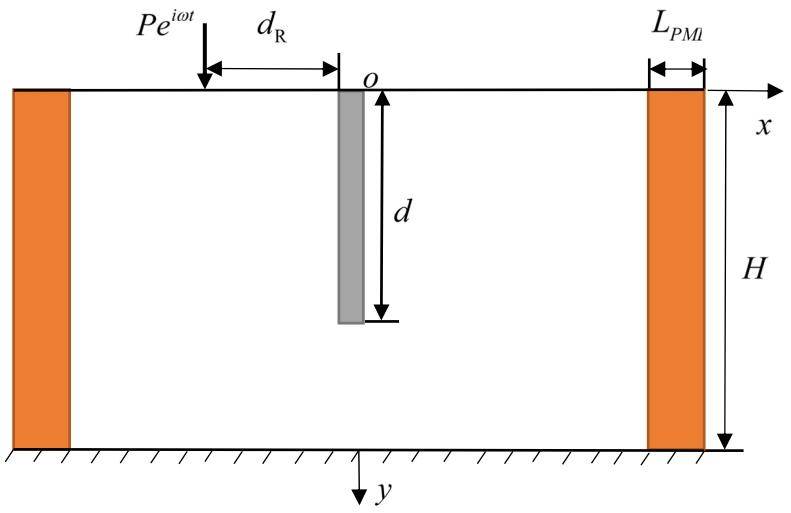

Fig 1. Schematic diagram of vibration isolation system

ISSN: 2414-1895 DOI: 10.6919/ICJE.202305_9(5).0029

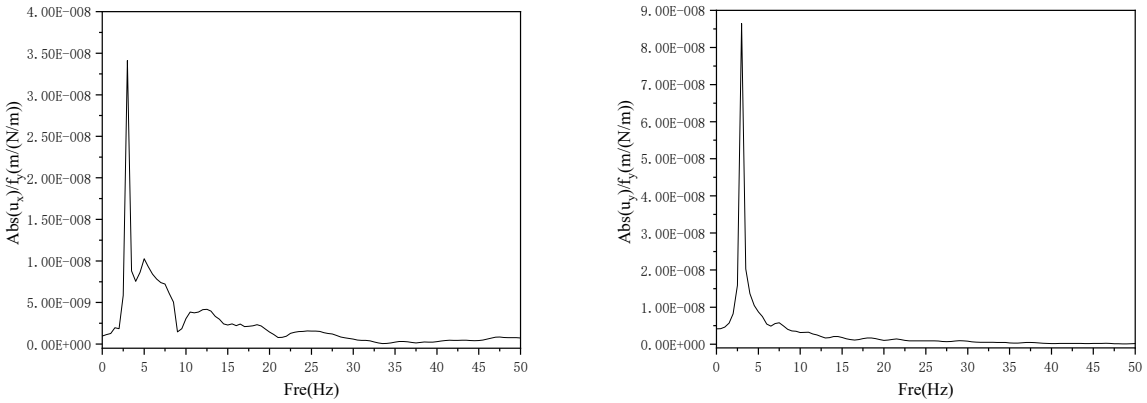

(a)vertical displacement ux (b)vertical displacement uy

Fig 2. WIB vibration isolation effect

4.2 The Influence of WIB Length on Vibration Isolation Effect

This section studies the influence of the length of the WIB on the vibration isolation effect. The bedrock is assumed to be rigid, and only one soil layer is assumed to be covered on the bedrock. The harmonic point load is (x, y) = (-6.5m, 0m), and the frequencies are 5Hz, 10Hz, and 20Hz respectively. The center abscissa of the WIB is 0m, and the length d of the WIB is 5m, 10m, and 15m respectively. The PML boundary is applied on both sides of the vibration isolation system, the outer boundary of PML is free, and the bottom of the system is fixed. The material and geometric parameters of the WIB and soil are shown in Table 1. Similarly, the shear modulus of WIB and soil is given by Cole-Cole model.

To evaluate the vibration isolation effect of the WIB, the amplitude reduction ratio is defined, that is, the ratio of the vertical displacement amplitude of the surface when the WIB exists to the vertical displacement amplitude of the surface when the WIB degenerates into soil.

$$A_r(\mathbf{x}_\perp) = \frac{\left|u_y^{(w)}(\mathbf{x}_\perp, y=0)\right|}{\left|u_y(\mathbf{x}_\perp, y=0)\right|}, \tag{18}$$

where $\left|u_y^{(w)}(\mathbf{x}_\perp, y=0)\right|$ and $\left|u_y(\mathbf{x}_\perp, y=0)\right|$ are the absolute values of the vertical displacement amplitudes at the point $\mathbf{x}_\perp$ on the soil surface in the presence and absence of the WIB. For a specific domain with the area S, the average $\overline{A}_r$ can be defined for the area [13]

$$\overline{A}_r = \frac{1}{S}\int_S A_r dS, \tag{19}$$

Fig.3 shows that increasing the length of the WIB can effectively improve the vibration isolation effect of the vibration isolation system. Fig.3(a) shows that when the load frequency is 5Hz, increasing the length of the WIB has a significant effect on improving the vibration isolation. Fig.3(b) shows that when the load frequency is 10 Hz, increasing the length of the WIB in a certain range can improve the vibration isolation effect of the WIB. At x = 10 m, the vibration isolation effect of the WIB with a length of 15 m is lower than that of the WIB with a length of 10 m. Figure 3 (c) shows that when the load frequency is 20 Hz, although increasing the length of the WIB can also improve the vibration isolation effect of the vibration isolation system, it is not as significant as when the load frequency is 5 Hz.

ISSN: 2414-1895 DOI: 10.6919/ICJE.202305_9(5).0029

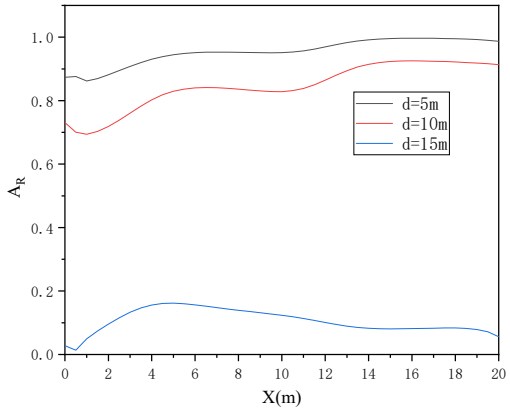

(a)5Hz

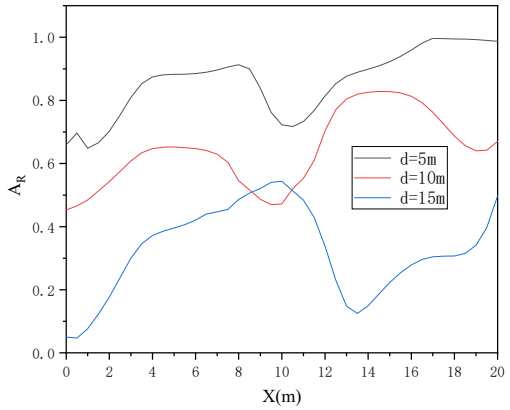

(b)10Hz

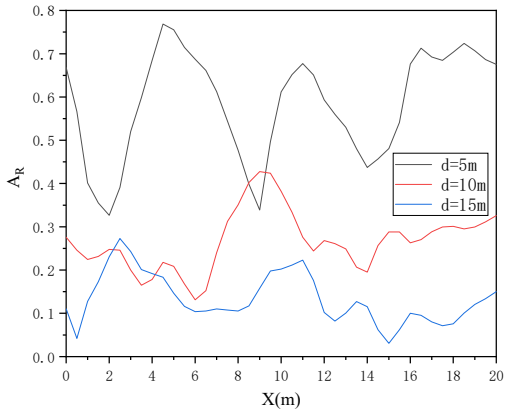

(c)20Hz

Fig 3. The influence of different length of wave blocking plate on the vibration isolation effect of vibration isolation system is compared.

4.3 The Influence of Modulus Ratio on the Vibration Isolation Effect of WIB

This section studies the influence of the modulus ratio of WIB and soil on the vibration isolation effect. The bedrock is assumed to be rigid, and only one soil layer is assumed to be covered on the bedrock. The harmonic point load is (x, y) = (-6.5m, 0m), and the frequencies are 5Hz, 10Hz, and 20Hz respectively. The center abscissa of the WIB is 0m. The shear modulus of the WIB is 1×10^9, 4×10^9, 1.2×10^{10}, and the ratio of shear modulus of wave resistance plate and soil are 50, 200, 600.The material and geometric parameters of the soil are shown in Table 1. Similarly, the shear modulus of WIB and soil is given by Cole-Cole model.

Fig.4 shows that increasing the shear modulus ratio of the WIB and the soil can improve the vibration isolation effect of the vibration isolation system. It can be seen from Fig.4 (a) that when the load frequency is 5 Hz, the vibration isolation effect of the vibration isolation system is closely related to the shear modulus ratio of the WIB and the soil, and the improvement of the vibration isolation effect is almost a multiple of the modulus ratio. It can be seen from Fig.4 (b) and (c) that when the load frequency is 10 Hz and 20 Hz, increasing the shear modulus ratio of the WIB and the soil can improve the vibration isolation effect of the vibration isolation system within a certain range, but not as significant as 5 Hz.

ISSN: 2414-1895 DOI: 10.6919/ICJE.202305_9(5).0029

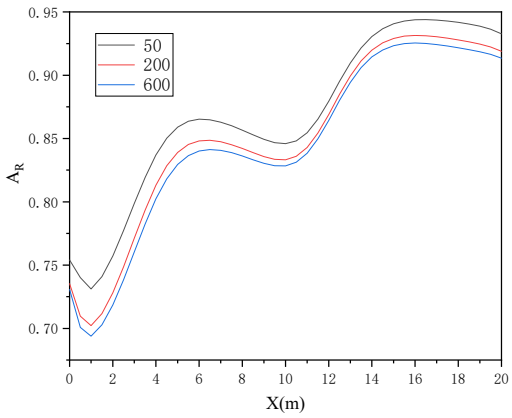

(a)5Hz

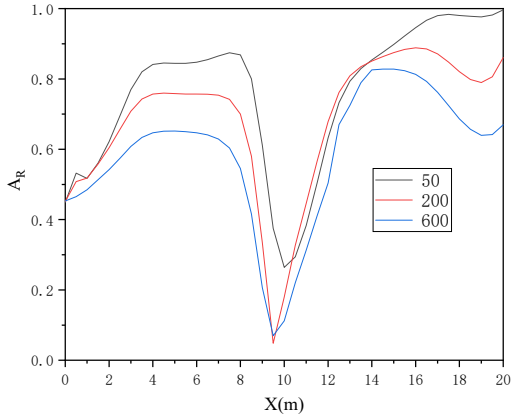

(b)10Hz

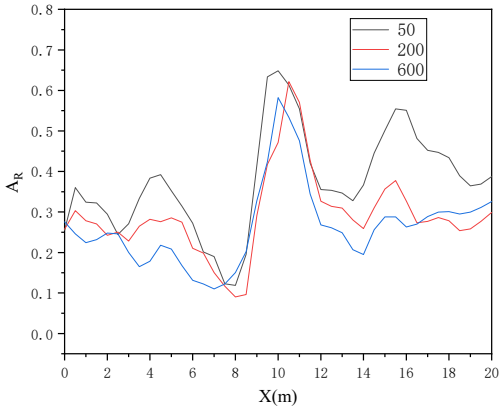

(c)20Hz

Fig 4. The influence of different wave resistance plate and soil shear modulus ratio on the vibration isolation effect of vibration isolation system is compared.

5. Conclusion

Based on the PML absorbing boundary, the frequency domain finite element model of the WIB vibration isolation system in the two-dimensional foundation is established, and the influence of various influencing parameters on the vibration isolation effect is analyzed. The main conclusions are as follows:

(1) The PML absorbing boundary can be easily combined with the finite element method to analyze the ground vibration isolation in the frequency domain. The vibration isolation effect is significant at low frequencies, and the vibration isolation effect is not as good as low frequencies at medium and high frequencies.

(2) The length of WIB has a significant effect on the vibration isolation system. Increasing the length of WIB can effectively improve the vibration isolation effect.

(3) The shear modulus ratio of WIB to soil also affects the vibration isolation system. Within a certain range, increasing the shear modulus ratio of WIB to soil can effectively improve the vibration isolation effect of the vibration isolation system.

Acknowledgments

Natural Science Foundation.

ISSN: 2414-1895 DOI: 10.6919/ICJE.202305_9(5).0029

References

[1] Chouw N, Le R, Schmid G. Propagation of vibration in a soil layer over bedrock [J]. Engineering Analysis with Boundary Elements, 1991, 8(3): 125-131.

[2] Schmid G, Chouw N, Le R. Shielding of structures from soil vibrations [J]. International Journal of Rock Mechanics and Mining Sciences and Geomechanics Abstracts, 1993, 30(4):651-662.

[3] Takemiya H, Fujiwara A. Wave propagation/impediment in a stratum and wave impeding block (WIB) measured for SSI response reduction [J]. Soil Dynamics and Earthquake Engineering, 1994, 13(1):49-61.

[4] Takemiya H, Hashimoto M, Shiraga A. Construction of wave impeding barrier (WIB column) for mitigation of traffic induced ground vibration [J]. Soil Mechanics and Foundation Engineering, 2002, 50 (9): 19-21.

[5] Takemiya H. Field Vibration Mitigation by Honeycomb WIB for Pile Foundations of a High-speed Train Viaduct [J]. Soil Dynamics and Earthquake Engineering.2004, 24(1):69-87.

[6] Peplow A T, Jones C, Petyt M. Surface vibration propagation over a layered elastic half-space with an inclusion [J]. Applied Acoustics, 1999, 56(4):283-296.

[7] Lombaert G, Degrande G, Franois S, et al. Ground-Borne Vibration due to Railway Traffic: A Review of Excitation Mechanisms, Prediction Methods and Mitigation Measures[J]. Notes on Numerical Fluid Mechanics and Multidisciplinary Design, 2015, 126:253-287.

[8] Celebi E, Goektepe F. Non-linear 2-D FE analysis for the assessment of isolation performance of wave impeding barrier in reduction of railway-induced surface waves [J]. Construction and Building Materials, 2012, 36:1-13.

[9] Thompson D J, Jiang J, Toward M, et al. Mitigation of railway-induced vibration by using subgrade stiffening[J]. Soil Dynamics and Earthquake Engineering, 2015, 79:89-103.

[10] Chew W C. Complex coordinate stretching as a generalized absorbing boundary condition [J]. Microwave and Optical Technology Letters, 1997, 15(6):363–369.

[11] Berenger J P. Three-Dimensional Perfectly Matched Layer for the Absorption of Electromagnetic Waves [J]. Journal of Computational Physics, 1996, 127(2):363-379.

[12] Cole KS , Cole RH . Dispersion and absorption in dielectrics[J]. Chemical Physics, 1941, 6:42-52.

[13] Woods RD. Screening of surface waves in soil. Journal of Soil Mechanics and Foundation Engineering 1968; 94: 407-435.